Review of experimental and theoretical status of the proton radius puzzle

Richard J. Hill[1,2,3,4,a]

[1] *Perimeter Institute for Theoretical Physics, Waterloo, ON, N2L 2Y5 Canada*
[2] *Fermi National Accelerator Laboratory, Batavia, Illinois 60510, USA*
[3] *TRIUMF, 4004 Wesbrook Mall, Vancouver, BC, V6T 2A3 Canada*

Abstract. The discrepancy between the measured Lamb shift in muonic hydrogen and expectations from electron-proton scattering and regular hydrogen spectroscopy has become known as the proton radius puzzle, whose most "mundane" resolution requires a $> 5\sigma$ shift in the value of the fundamental Rydberg constant. I briefly review the status of spectroscopic and scattering measurements, recent theoretical developments, and implications for fundamental physics.

1 Introduction

The so-called proton radius puzzle is the 5.6σ discrepancy between the proton electric charge radius $r_E^p = 0.8751(61)$ measured from a combination of electron scattering and (regular, electronic) hydrogen spectroscopy [1], and the radius $r_E^p = 0.84087(26)(29)$ measured from muonic hydrogen spectroscopy [2].[1] [2]

The large size of this discrepancy and its surprising appearance in seemingly well-known systems, have motivated numerous theoretical and experimental efforts across particle, nuclear and atomic physics. This talk begins by outlining the experimental basis for the puzzle in Sec. 2. Section 3 then describes theoretical issues that have received scrutiny since the emergence of the puzzle, and Sec. 4 describes some emerging experimental clues. Section 5 describes a few of the broader implications of the puzzle, and of work that has been motivated by the puzzle. Section 6 provides an outlook.

2 Outline of the puzzle

The hydrogen spectrum depends on the Rydberg constant R_∞ and the proton charge radius r_E^p, schematically as [3]

$$E_{n,\ell} \sim -\frac{R_\infty}{n^2} + \delta_{\ell 0}\frac{\left(r_E^p\right)^2}{n^3}\,, \tag{1}$$

---

[a] e-mail: richardhill@perimeterinstitute.ca
[1] These numbers correspond to the CODATA 2014 adjustment of constants, and the updated 2013 CREMA analysis. The CODATA 2010 value from electron measurements [4], $r_E^p = 0.8775(51)$, and the original 2010 CREMA analysis [5], $r_E^p = 0.84184(36)(56)$, yielded a discrepancy of 6.9σ.
[2] For earlier reviews, see Refs. [6, 7].
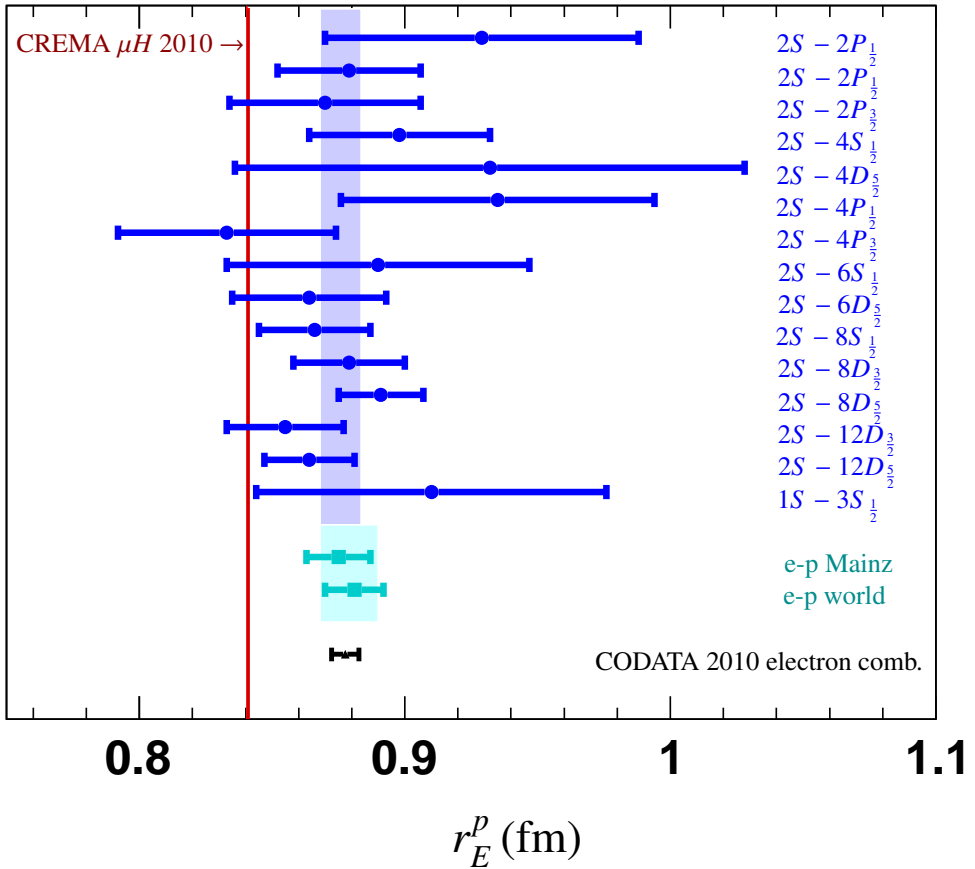
Figure 1. Status of the proton radius puzzle circa 2010. Blue data points denote various hydrogen intervals that are combined with the $1S - 2S$ interval to solve for r_E^p (datapoints as in Ref. [8]); blue band is the hydrogen average from Ref. [4]. Cyan data points are electron-proton scattering determinations circa 2010 from Mainz A1 collaboration data [9] and from other world data [10]; cyan band is the electron-proton scattering average from Ref. [11]. The black data point represents the 2010 CODATA [4] combination of hydrogen and electron-proton scattering determinations. The vertical red band is the 2010 CREMA determination from muonic hydrogen [5].

where $E_{n,\ell}$ is the energy for state of principle and angular quantum numbers n, ℓ. The uncertainty on r_E^p, as presently determined by electron-proton scattering and hydrogen spectroscopy, limits the precision for R_∞ that can be obtained using Eq. (1) and the precisely measured 1S-2S hydrogen interval [13, 14]. One motivation to measure the Lamb shift (i.e., the 2P-2S interval) in muonic hydrogen is that it can provide a precise determination of r_E^p, and hence a more precise determination of R_∞. The surprising result in 2010 from the CREMA collaboration was a determination of the Lamb shift [5]

with an inferred charge radius not only much more precise than, but in sharp tension with, results from both regular hydrogen spectroscopy and electron-proton scattering. Correspondingly, the Rydberg constant determined using the charge radius inferred from the Lamb shift was in sharp tension with previous determinations. The measurements representing the proton radius puzzle, circa 2010, are displayed in Fig. 1.

3 Status of some theory issues

I summarize here some recent progress regarding theoretical issues impacting the proton radius puzzle. I focus on the issues of form factor nonlinearities and radiative corrections in electron-proton scattering; and in higher-order proton structure effects in muonic hydrogen.

3.1 Electron-proton scattering: theory issues

The proton charge radius is defined by the slope of the electric charge form factor of the proton:

$$\frac{1}{6}\left(r_E^p\right)^2 \equiv \frac{d}{dq^2}\bigg|_{q^2=0} G_E^p(q^2)\,,\tag{2}$$

where $q^2 = -Q^2$ is the invariant momentum transfer of the scattering process. Two important issues surrounding the determination of the charge radius from scattering data are the treatment of form factor nonlinearities, and the treatment of radiative corrections.

3.1.1 Form factor nonlinearities

Figure 2 illustrates an essential feature of fits to electron-proton scattering data. Since the radius is defined by the slope of the form factor, Eq. (2), a finite range of momentum transfer must be included. Care must then be taken to account for nonlinearities in form factor shape. In fact, the situation is more dire than simply needing to account for higher-order terms in the Q^2 Taylor expansion of G_E^p: in order to obtain relevant precision with current data (i.e., with an error small compared to the $\sim 0.034\,\mathrm{fm}$ radius anomaly) the required Q_{max}^2 is larger than the radius of convergence for the form factor!

Happily, this problem is readily solved: as illustrated in Fig. 3, a variable change mapping the cut plane onto the unit circle ensures convergence of a Taylor expansion in the new variable throughout the entire domain of analyticity:[3]

$$G_E^p(q^2) = \sum_{k=0}^{\infty} a_k [z(q^2)]^k\,,\qquad z(q^2) = \frac{\sqrt{t_{\mathrm{cut}} - q^2} - \sqrt{t_{\mathrm{cut}} - t_0}}{\sqrt{t_{\mathrm{cut}} - q^2} + \sqrt{t_{\mathrm{cut}} - t_0}}\,.\tag{3}$$

Moreover, the expansion is systematically improvable, and the error due to truncating the expansion at a given order is reliably estimated.[4]

A range of parameterizations has been used to describe the elastic vector form factors of the proton.[5] In many cases, these parameterizations are in conflict with known properties of the form factors inherited from QCD. For example, as discussed around Fig. 2, a Taylor expansion around $q^2 = 0$ is

---

[3]Formalism for z expansion and nucleon form factors is described in Refs. [16, 17], and several applications are found in Refs. [15, 18–20]. Related formalism and applications may be found in [21–37].

[4] The maximum size of $|z(q^2)|$ is bounded in a given kinematic window, and the coefficients a_k are dimensionless order unity numbers.

[5] For a discussion and references, see Ref. [16].
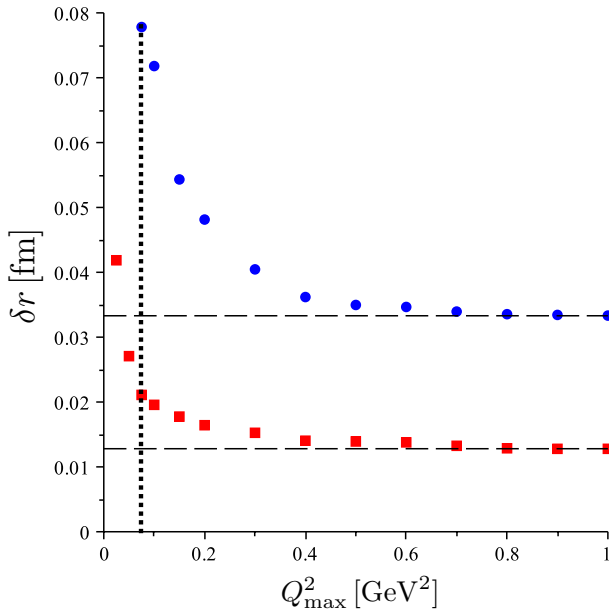
Figure 2. Statistical error on r_E^p as a function of the maximum momentum transfer retained in the fit, Q_{max}^2, for the 1422 point A1 MAMI dataset (red squares) and for the complementary world cross section and polarization dataset (blue circles). The horizontal dashed lines are large-Q_{max}^2 asymptotes. The vertical dotted line represents the limit $Q_{max}^2 = 4m_\pi^2$ beyond which the two-pion threshold introduces nonanalytic structure. For details, see Ref. [15].

valid only up to $q^2 = 4m_\pi^2$ where pion production in the crossed channel corresponds to a branch point singularity. As another example, a Padé approximation of continued fractions can be justified only when the spectral function appearing in the dispersive representation of the form factor, $\mathrm{Im}\,G_E(q^2)$, is positive definite.[6] Such parameterizations, with sufficiently many parameters, may be able to fit the available data. However, without a priori control over the number of relevant parameters, there is an inevitable arbitrariness in deciding how many parameters to keep, and a complicated analysis is required to understand the interplay with statistical and systematic experimental errors.

With theoretical control over form factor nonlinearities, we may revisit the extraction of the charge radius from scattering data. Figure 4 shows several steps in a reanalysis of the 1422 point Mainz A1 dataset (see Ref. [15], Table XIV). The topmost point ("A1 spline") displays the original A1 analysis result,[7] employing the entire Q^2 range (up to $1\,\mathrm{GeV}^2$) and a cubic spline fit [40]. The next point ("Bounded z exp.") displays the corresponding result using precisely the same data and errors as the first point, but replacing the spline parameterization by the z expansion [with standard statistical priors on the coefficients a_k in Eq. (3)]. The next four points show the impact of using a more conventional radiative correction model ("+ Hadronic TPE"); rebinning data taking at identical kinematics ("Re-

---

[6] A positive spectral function would predict an asymptotic scaling at large momentum transfer $\sim 1/Q^2$, in conflict with the known $\sim 1/Q^4$ behavior. For an application where this positivity condition *is* satisfied, see Ref. [38].

[7] As discussed in Ref. [15], this results from adding different systematic errors linearly [39], compared to the quadrature sum advocated in Ref. [40].
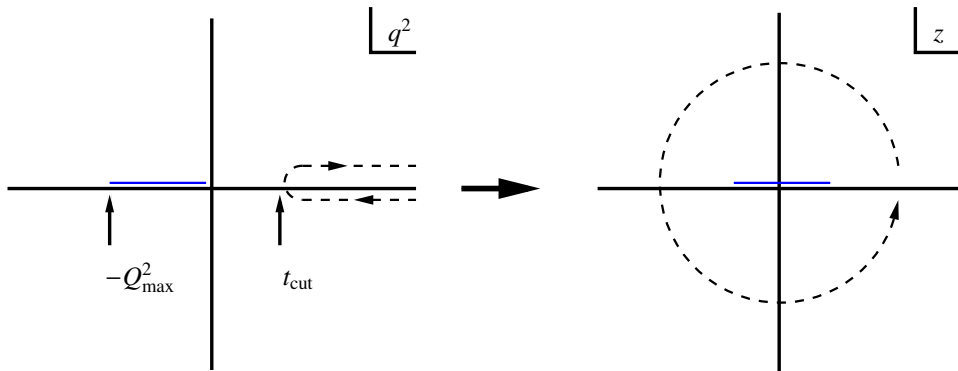
Figure 3. Variable transformation $q^2 \to z(q^2)$ mapping the cut plane to the unit circle. The physical region for spacelike scattering, denoted in blue, is $-Q^2_{max} < q^2 < 0$. The singularity corresponding to pion production in the crossed channel is $t_{cut} = 4m^2_\pi$.

bin, 0.3%-0.4% syst.");[8] including a larger error budget to account for known sources of correlated systematics ("+0.4% corr. syst."); and choosing $Q^2_{max} = 0.5\,\text{GeV}^2$ to maximize radius sensitivity but minimize potential large-Q^2 systematics (cf. Fig. 2). The final point in the figure displays the result of a similar analysis applied to other world data (not including the Mainz A1 dataset). It is readily seen that form factor shape assumptions can have dramatic consequences for radius extractions.

The decomposition of the high statistics Mainz A1 collaboration dataset [40] into subsets with independent floating normalization parameters has been used to minimize the impact of poorly-measured systematic effects that primarily impact overall cross section normalization. A variant of this analysis in Ref. [15] has been used to quantify how large a missing or mismodeled systematic effect would need to be in order to impact the radius extraction. In short, there would need to be: a variation larger than $\sim 0.4\%$ over data subsets;[9] or a variation of a more extreme functional form than those considered; or unaccounted correlations between different subset variations.

Figure 5 displays the dependence of the extracted radius on the range of Q^2 considered. There is mild tension between fits to the entire Q^2 range below $1\,\text{GeV}^2$, and fits restricted to low-Q^2. While not of high statistical significance, the appearance of a similar feature in fits to independent datasets may be suggestive a common theoretical systematic. It does not escape attention that the low-Q^2_{max} fits have central r^p_E value closer to the r^p_E from muonic hydrogen (albeit with large error). Moreover, radiative corrections are known to be enhanced at large Q^2, owing to large logarithms, $\sim \log(Q^2/m^2_e)$ in the perturbative expansion. Let us revisit the status of these corrections.

3.1.2 Radiative corrections

Here I review the definition of the charge radius in the presence of QED radiative corrections, and discuss the status of soft and hard radiative corrections to the scattering process.

The definition (2) assumes a choice for Born form factor.[10] In modern effective field theory language, G_E is the hard contribution in the factorization formula for the onshell form factor. It should be noted that a number of different conventions exist in the literature for defining the radius when

---

[8] The rescaling analysis by which kinematically uncorrelated systematic errors were estimated in Ref. [40] would otherwise unintentionally drive these errors to zero with repeated measurements at the same kinematics.

[9] The data is divided into 18 subsets corresponding to combinations of beam energy and spectrometer configuration.

[10] For a discussion of definitions including QED radiative corrections, see Appendix B of Ref. [41].
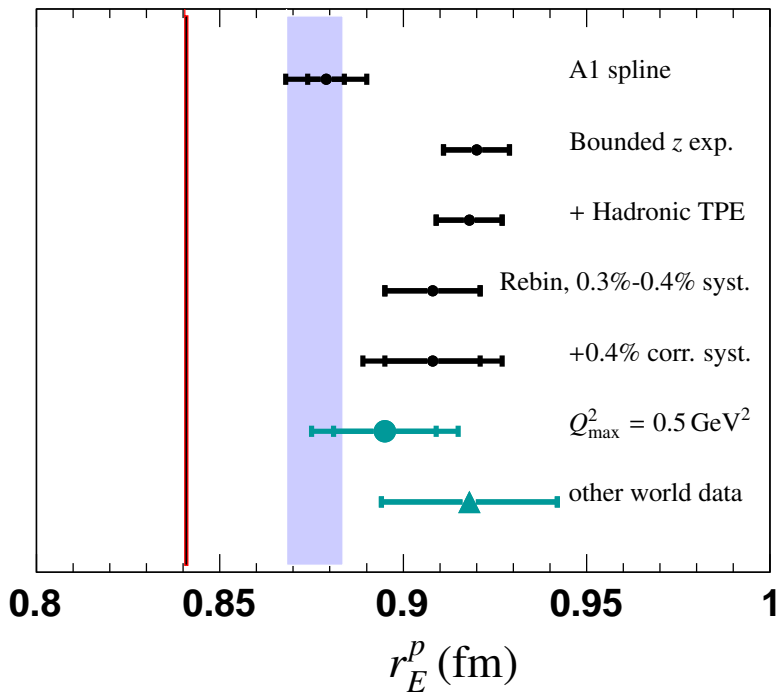
Figure 4. Radius extraction from 2010 Mainz A1 collaboration data. The topmost point is the original A1 analysis for reference. The next five points represent z expansion fits under a series of modifications as described in the text, culminating in the final result given by the large cyan circle. The final point (large triangle) represents the same analysis applied to other world data. From Table XIV of Ref. [15]. The vertical blue and red bands are the regular hydrogen and muonic hydrogen results reproduced from Fig. 1.

accounting for radiative corrections. The convention advocated in Refs. [41, 42] is defined by the $\overline{\text{MS}}$ renormalization scheme for the soft function, and has the property that the radius for a point particle vanishes in the presence of first order radiative corrections.

The complete cross section for the elastic scattering process including radiative corrections may be written,

$$d\sigma \propto H \times J \times R \times S \equiv H(\mu = M) \times (1 + \delta), \tag{4}$$

where H (hard contribution) is defined to contain the Born form factors and hard TPE, and the J (jet), R (remainder) and S (soft) factors are calculable in QED. In the latter equality we have defined the scheme choice for H (at factorization scale $\mu = M$), and defined the radiative correction factor δ appearing in Fig. 7.

The product JRS in Eq. (4) contains large logarithms, $L \sim \log Q^2/m_e^2$. For typical scattering kinematics, the argument of the logarithm involves ratios of GeV to MeV scales. Leading corrections are as large as $\sim 30\%$, and naively subleading corrections must also be included. In previous analyses, an exponentiation ansatz has been employed [40, 43] to account for logarithmically enhanced terms at
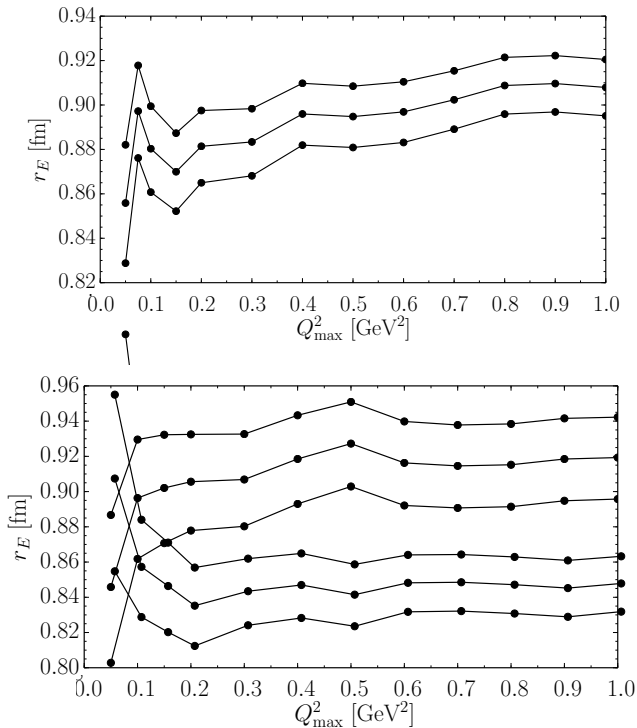
Figure 5. Proton electric charge radius as a function of maximum Q^2 retained in the fit to scattering data. The three curves represent central values and 1σ error bars. Top: 2010 Mainz A1 dataset (statistical and uncorrelated systematic errors only). Bottom: other world data. From Ref. [15].

second- and higher-order in perturtabive QED. This procedure fails to capture subleading logarithms, beginning at order $\alpha^2 L^3$. The potential impact of such subleading corrections is illustrated in Fig. 6, top, where an effective renormalization scale variation is represented by the blue lines. Clearly, corrections beyond the leading terms must be controlled in order to exhibit a discrepancy between the scattering data (black solid line) and muonic hydrogen (red dotted line).

The factor H in Eq. (4) contains the hard two-photon exchange contribution, which must be subtracted in order to isolate the Born form factors of interest. Figure 6, bottom, displays the radius extracted using several models for the hard contribution to TPE [44–49]. The variation between red line (no hard correction) and other lines shows that the total hard TPE contribution enters at a level comparable to the proton radius anomaly. Clearly this contribution must also be reliably controlled.

Figure 7, LHS, shows the complete calculation of the radiative correction factor δ [41] for an illustrative kinematic point, displaying convergence of leading logarithms (red), next-to-leading logarithms (blue) and a complete next-to-leading order calculation (black). Figure 7, RHS, shows the same complete calculation (black) compared to the previously-employed exponentiation ansatz (red). The difference between black and red curves is the impact of subleading logarithms missing in the exponentiation ansatz.
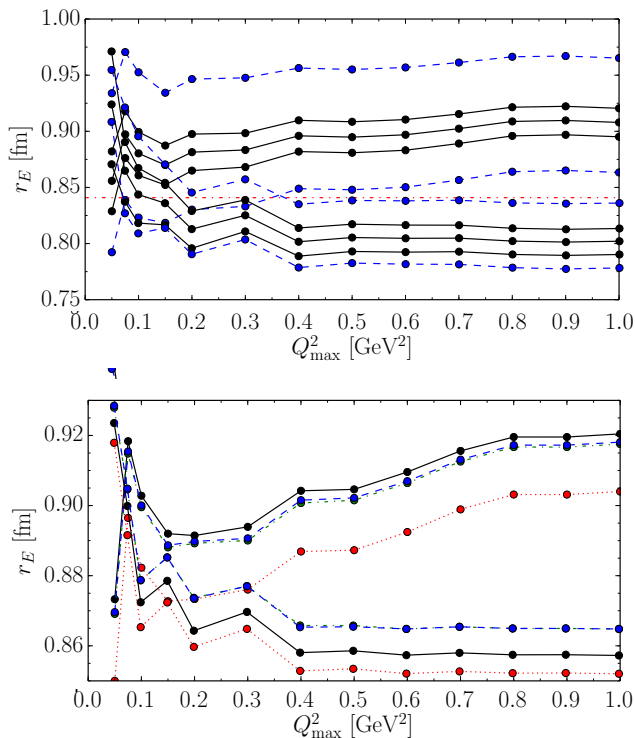
Figure 6. Potential impact of radiative corrections. Top: black solid lines are from the top plot of Fig. 5. The blue dashed lines represent an error band from factorization scale variation in the radiative corrections, where only leading logarithms are controlled. The red dotted line is the central value from muonic hydrogen. Bottom: the bottom, red, dotted line is the radius extracted with vanishing hard TPE correction. The remaining lines are results using different models for hard TPE. From Ref. [15].

In previous work employing the exponentiation ansatz, there is an implicit choice of conflicting renormalization scales in the one-photon exchange and two-photon exchange contributions that results in an ambiguity between the red and blue lines in Fig. 7.[11] The difference between the red and blue curves is an (indirect) measure of hard TPE model uncertainty.

These modifications to the radiative corrections impact cross sections at the $\sim 0.5 - 1\%$ level over the kinematics of the A1 experiment. While this is in tension with the assumed error budget of $\sim 0.1 - 0.2\%$, a large part of the correction will be absorbed by floating normalization parameters.

3.1.3 Interplay with other constraints

A variety of alternative assumptions regarding fit functions and data selections have been employed in the literature to extract the charge radius from scattering data (for an incomplete survey, see Refs. [18, 50–58]). Several analyses argue for a small radius obtained by retaining only the low-Q^2 scattering data. As Fig. 2 shows, inclusion of only low-Q^2 data (e.g., where a Taylor expansion is appropriate)

---

[11]In particular, the usual convention for Born form factors corresponds to the scale choice $\mu = M$, M the proton mass, while the usual (Maximon-Tjon) convention for hard TPE corresponds to the choice $\mu = Q$.
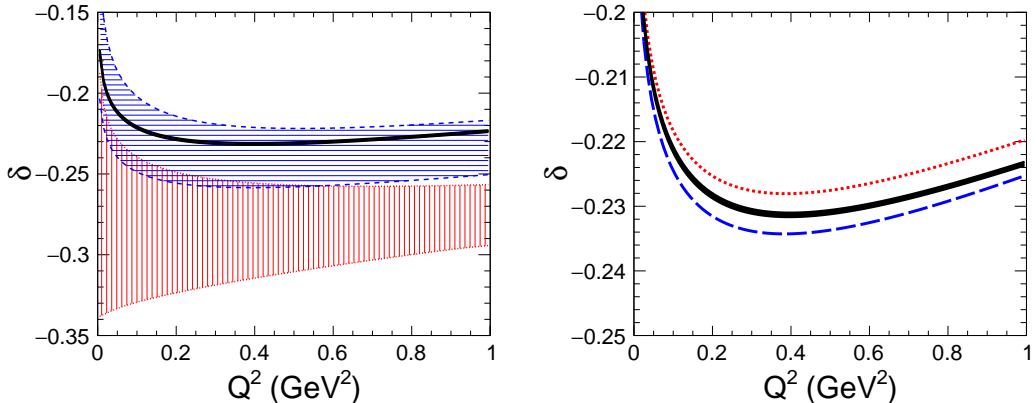
Figure 7. Radiative correction factor δ in Eq. 4, at electron energy $E = 1\,\text{GeV}$ and bremsstrahlung cut $\Delta E = 5\,\text{MeV}$. LHS: red vertical hashed, blue horizontal hashed, and black solid bands represent leading logarithm, next-to-leading logarithm and next-to-leading order calculations. RHS: black is the same as LHS; red dotted and blue dashed give two versions of the previously-employed exponentiation ansatz. From Ref. [41].

cannot achieve sufficient precision to address the proton radius puzzle without further information.[12] Beyond the question of statistical power, such an approach must assume that any systematic impacting higher-Q^2 data does not invalidate the lower-Q^2 data.

Isospin decomposition of electron-proton and electron-neutron data can be used to place somewhat tighter constraints on the form factors [16, 59], since the isoscalar threshold is larger: phrased in terms of z expansion, the larger threshold, $(3m_\pi)^2$ versus $(2m_\pi)^2$, implies a smaller maximum size of $|z(q^2)|$, and faster convergence with fewer relevant expansion coefficients [16]. Fits to the combined proton and neutron data, together with $\pi\pi \to N\bar{N}$ constraints, have been argued to imply a smaller value of r_E^p. However, this conclusion relies on modeling the spectral function at inaccessible kinematics.[13] Beyond the question of model-dependence in the spectral functions, a result consistent with muonic hydrogen again would demand that the scattering data be effectively overruled by other constraints or assumptions.

3.2 Muonic hydrogen: theory issues

Muonic hydrogen is much more sensitive to proton structure than ordinary hydrogen, due to the huge wavefunction enhancement,

$$\frac{|\psi_{\mu H}(0)|^2}{|\psi_{eH}(0)|^2} \sim \frac{m_\mu^3}{m_e^3} \sim (200)^3 . \tag{5}$$

Relative to the leading $\sim m_\ell \alpha^2$ contribution, proton structure impacts the muonic hydrogen spectrum $\sim (200)^2$ times more strongly than regular hydrogen.

---

[12] Reference [57] argues to supplement the low-Q^2 scattering data with constraints on curvature and higher-order derivatives of the form factor from chiral perturbation theory.

[13] See for example, Ref. [16], where inclusion of the model-independent part of the spectral function reduces uncertainty but does not dramatically alter the central value of the radius extracted from the considered data. For recent analysis, see also Ref. [60].
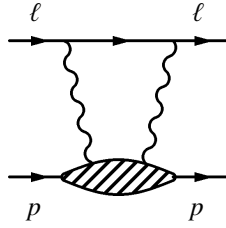
Figure 8. Two photon exchange contribution to forward scattering $\ell p \to \ell p$, where $\ell = e, \mu$.

In addition to the radius, other proton structure effects enter, in particular two-photon exchange contributions. The matching condition from a relativistic QCD theory of quarks and gluons onto the low energy Hamiltonian is represented by the box diagram of Fig. 8, which is given by an integral over the forward Compton amplitude of the proton. The relevant proton structure is contained in the spin-averaged Compton amplitude, described by two invariant amplitudes, $W_i(\nu, Q^2)$, $i = 1, 2$. These amplitudes are determined by elastic and inelastic scattering data using dispersion relations. However one of the dispersion relations does not converge, and requires a subtraction,

$$
W_1(\nu, Q^2) = W_1(0, Q^2) + \frac{\nu^2}{\pi} \int_0^\infty d\nu'^2 \, \frac{\mathrm{Im} W_1(\nu', Q^2)}{\nu'^2(\nu'^2 - \nu^2)} ,
$$

$$
W_2(\nu, Q^2) = \frac{1}{\pi} \int_0^\infty d\nu'^2 \, \frac{\mathrm{Im} W_2(\nu', Q^2)}{\nu'^2 - \nu^2} . \tag{6}
$$

The subtraction term, $W_1(0, Q^2)$ is a major source of uncertainty, since it is not directly determined by scattering data.
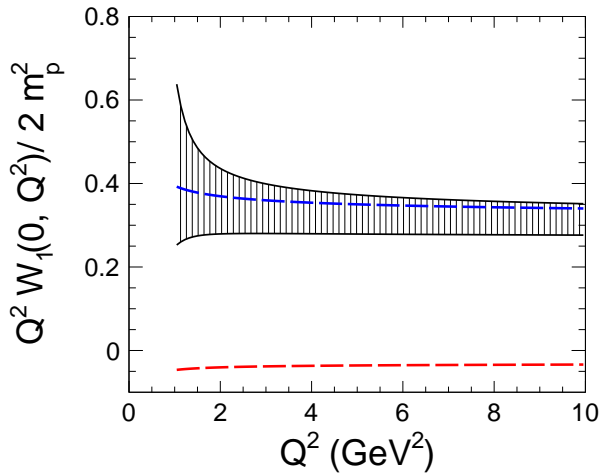
Figure 9. Leading OPE prediction for $W_1(0, Q^2)$. The bottom red dashed line, and top blue dashed line represent central values of the spin-0 and spin-2 contributions. The hatched band represents the total including perturbative and hadronic uncertainty. From Ref. [61].

The subtraction function can be computed in various regimes. At low $Q^2 \ll m_\pi^2$ the Taylor expansion of $W_1(0, Q^2)$ is determined by Wilson coefficients of NRQED [42]; these coefficients are in turn determined by data or by nonperturbative QCD calculations.
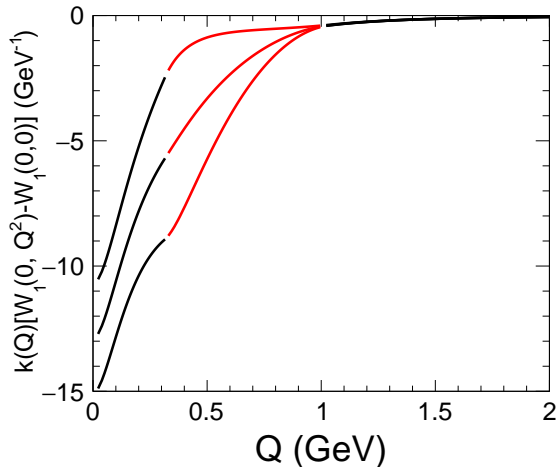
Figure 10. Contribution of the subtraction function $W_1(0, Q^2)$ to the two-photon exchange effect in the muonic hydrogen Lamb shift. The black lines on the LHS and RHS of the plot show central value and error band for the low-Q^2 (NRQED) and high-Q^2 (OPE) regions. The red lines in the intermediate region are interpolations. The energy shift is proportional to the area under the curve. From Ref. [61].

At high $Q^2 \gg m_p^2$, $W_1(0, Q^2)$ can be computed using operator product expansion (OPE),

$$W_1(0, Q^2) = \frac{2m_p^2}{Q^2} A(Q^2) + O(1/Q^4) \,, \tag{7}$$

where $A(Q^2)$ is a product of perturbatively calculable coefficients and nucleon matrix elements of local operators. The complete result for the leading OPE contains contributions from both spin-0 and spin-2 operators. Previous investigations of the impact on the muonic hydrogen TPE have assumed subtraction functions without the correct large-Q^2 behavior. For example, Refs. [62, 63] consider an interpolation formula that identifies $A(Q^2)$ with low-energy quantities. Reference [64] adopts a result in the literature [65] for $A(Q^2)$ that contains the incorrect spin-0 contribution and entirely omits the numerically dominant spin-2 contribution. An extrapolation using for the first time the correct low-Q^2 and high-Q^2 constraints is displayed in Fig. 10.

Additional information on $W_1(0, Q^2)$ in the regime $m_\pi^2 \lesssim Q^2 \ll m_p^2$ can be obtained from chiral lagrangian analysis. A sample result is displayed in Fig.11, where the LHS compares different orders in the chiral expansion, and the RHS gives the analog of Fig. 10. It should be noted that these curves perform a conventional separation of $W_1(0, Q^2)$ into a piece determined by elastic form factors (denoted by $W_1(0, Q^2)^{\text{SIFF}}$ in Fig. 11, and for simplicity here assumed to have zero uncertainty), and a remainder. Uncertainties related to this separation are not contained in curves displayed in Fig. 11.

Fig. 12 displays results in the literature for the TPE contribution to the muonic hydrogen Lamb shift, including the results corresponding to Figs. 10 and 11. The TPE contribution remains a dominant source of uncertainty on the r_E^p extraction from muonic hydrogen.
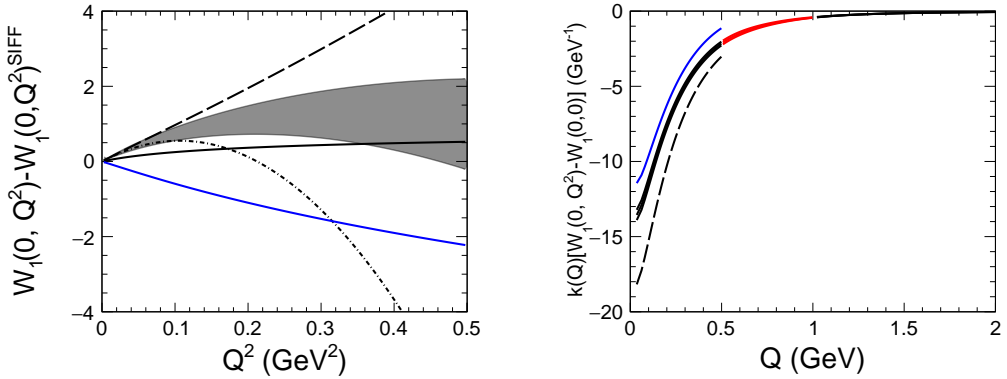
Figure 11. Contribution of subtraction function to two-photon exchange, using hadronic calculation of Birse and McGovern [62]. LHS: $W_1(0, Q^2)$ using "third order", "fourth order" and "fourth order plus Δ" results from Ref. [62] (black solid line, black dashed line, solid band); "fourth order plus Δ" Taylor expanded through $O(Q^4)$ (dash-dotted black line); "third order" result from the relativistic formulation of Ref. [70]. RHS: same as Fig. 10 but using the gray band on LHS for $W_1(0, Q^2)$ [at fixed $W_1(0, Q^2)^{\text{SIFF}}$]. Plots from Ref. [61].
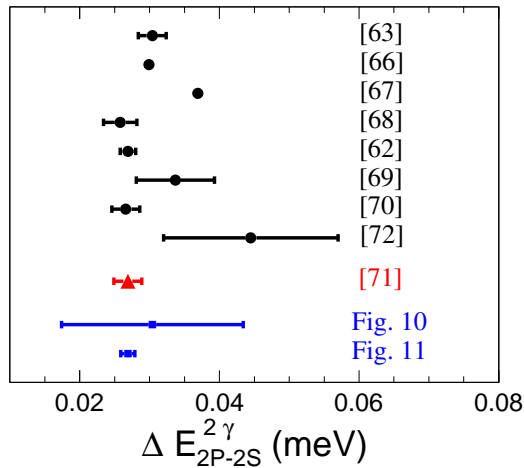
Figure 12. Two-photon contribution to the Lamb shift in muonic hydrogen, adjusted to common proton elastic form factors (see text). The red triangle is the summary of Ref. [71] used in the 2013 CREMA muonic hydrogen extraction of r_E^p. Plot from Ref. [61].

4 New experimental clues

There are several directions of activity to better understand the proton radius puzzle.

4.1 New muonic atom measurements

The Lamb shift in muonic deuterium has been measured in Ref. [73]. Combined with the regular hydrogen-deuterium isotope shift of the 1S-2S transition [12], this result has been translated to a

value

$$r_E^p(\mu D) = 0.83562(21)\,\text{fm}\,. \tag{8}$$

Further new measurements are anticipated [74] in muonic ^{3}He and ^{4}He, where nuclear structure effects are important for interpretation [75–77].

4.2 New regular hydrogen measurements

It may be noted that no single measurement in regular hydrogen differs from the muonic hydrogen line in Fig. 1 by more than $\sim 2\sigma$, raising the question of how to properly average these results.[14] New preliminary results for the hydrogen $2S - 4P$ splitting have been reported by Beyer et al. [8, 78], with a "small" radius, and error comparable to the existing hydrogen average. In the absence of a final result, Fig. 13 displays the anticipated radius sensitivity,[15] with central value taken for illustration as the CODATA 2014 electron combination. For an overview of other potential regular hydrogen measurements see Ref. [79]. A range of new measurements with hydrogen-like He$^+$ ions [80–82], molecules and molecular ions [83–87], and circular Rydberg states [88, 89] are also anticipated.[16]

4.3 Low-Q^2 electron-proton scattering

Form factor nonlinearities can be theoretically controlled, provided that experimental errors and correlations are precisely specified. However, it is interesting to extract the proton charge radius entirely from low-Q^2 data, especially given the apparent tension between low-Q^2 and high-Q^2 data illustrated in Fig. 5. The PRad experiment at JLab [90] utilizes a non-magnetic spectrometer, a windowless target, and a simultaneous calibration with Møller scattering to control experimental systematics. First data was collected in May/June 2016, and a first analysis is anticipated in 2017. Fig. 13 displays the anticipated radius sensitivity,[17] with central value taken for definiteness as the CODATA 2014 electron combination. Low-Q^2 data have also been collected using the initial state radiation (ISR) technique at MAMI [91]. An experiment with a new target is being planned that will reduce backgrounds and access $Q^2 \sim 10^{-4}\,\text{GeV}^2$.

4.4 Muon-proton scattering

As illustrated in Fig. 1, both bound state and scattering measurements exist for the electron system. Only a bound state measurement exists for the muon system. A measurement of the proton charge radius from muon-proton elastic scattering has been proposed by the MUSE collaboration [92]. A combination of $e^\pm$ and $\mu^\pm$ data should provide cancellation of systematic errors and empirical constraints on two-photon exchange. Fig. 13 displays the anticipated radius sensitivity,[18] with central value taken for illustration as the previous muonic hydrogen average.

---

[14] For a discussion, see Ref. [8].

[15] An uncertainty 0.010 fm has been assumed in the figure.

[16] For further discussion see Ref. [3].

[17] A 1% radius uncertainty is assumed in the figure.

[18] An uncertainty 0.010 fm for the radius determined from muon scattering has been assumed in the figure. The difference between radii from electron and muon scattering should have smaller uncertainty.
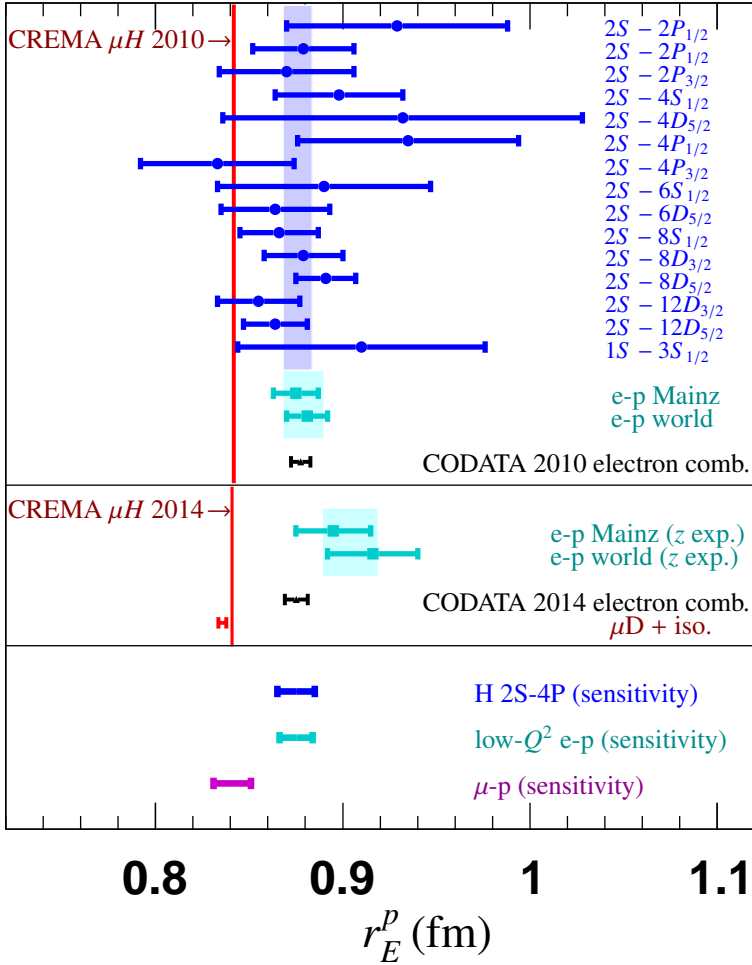
Figure 13. Status of the proton radius puzzle circa 2016, with prospects for new data. The upper pane is reproduced from Fig. 1. The middle pane shows updated results. The cyan points give updated fits to electron scattering data using z expansion (final two points in Fig. 4, from Ref. [15]. The black point represents the 2014 CODATA [1] combination of hydrogen and electron-proton scattering determinations. The red point is from the 2016 CREMA muonic deuterium Lamb shift measurement using the regular hydrogen-deuterium isotope shift [73]. The bottom pane shows expected sensitivities of anticipated results in: regular hydrogen [78] (blue); low-Q^2 electron-proton scattering [90] (cyan); and muon-proton scattering [92] (magenta). See text for details.

4.5 Summary of status and prospects

Figure 13 displays the current status of the proton radius puzzle. Compared to Fig. 1, the muonic hydrogen error bar has been increased to reflect updates and a revised treatment of TPE in Ref. [71], and the new muonic deuterium data point has been included. The electron scattering results reflect the treatment of form factor nonlinearities and more conservative systematic errors from Ref. [15]. In

addition to these existing results, projected sensitivities are illustrated for the $2S - 4P$ measurement in regular hydrogen; low-Q^2 electron-proton scattering; and muon-proton scattering.

5 Some broader implications

Regardless of its resolution, the proton radius puzzle has acted as a "disruptive technology", highlighting critical areas where better understanding is needed, ranging from precision measurements and fundamental constants to neutrino physics and formal questions in effective field theory.

5.1 Nucleon form factors for neutrinos and other processes
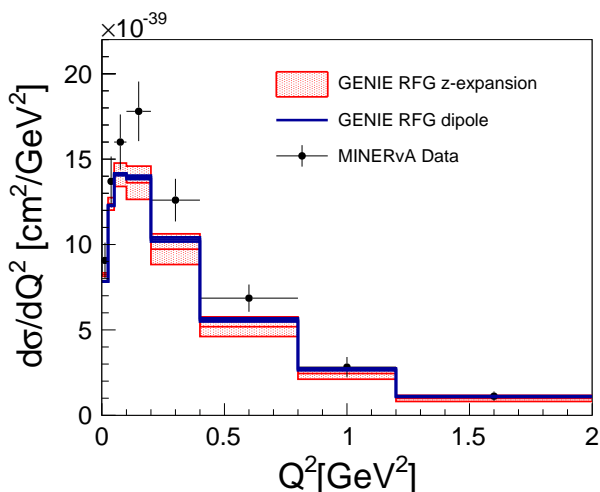
Figure 14. Comparison of experimental data from the MINERvA collaboration [94] with the theory prediction in a simple nuclear model, showing error induced by nucleon-level form factors. The previously underestimated uncertainty is in blue, the updated uncertainty is in red. From Ref. [95].

The elastic form factors of the nucleon are precisely defined quantities that impact many observables. The proton radius puzzle has emphasized the importance of properly accounting for form factor shape uncertainty and radiative corrections in the analysis of experimental data. An important application of current relevance is neutrino-nucleus scattering at long baseline oscillation experiments.[19] At the nucleon-level, the basic signal process for neutrino detection is charged-current quasielastic scattering, $\nu_\ell n \to \ell^- p$. Figure 14 illustrates that with proper treatment of form factor shape, the nucleon-level uncertainty on the cross section is an order of magnitude larger than previously thought.[20] This complicates the program of constraining nuclear effects from measurement: for example, in Fig.14,

---

[19] Another recent application is to the study of photon initiated processes at the LHC [93].

[20] Reference [95] determines $r_A^2 = 0.46(22)\,\mathrm{fm}^2$ from existing data. Other results in the literature quote much smaller uncertainty, for example Ref. [96] finds $r_A^2 = 0.454(12)\,\mathrm{fm}^2$. This small uncertainty arises from a dipole shape assumption that was applied to neutrino scattering and pion electroproduction data [96]. Taken at face value, the uncertainty on the axial radius would be *smaller* than the uncertainty on scattering determinations of the proton electric charge radius, even though the former results from small statistics neutrino beams with poorly known flux on nuclear targets (vs. high statistics electron beams of monoenergetic energy on proton targets).

the data-theory discrepancy is due to a combination of nucleon-level input uncertainty and nuclear modeling error. As a quantitative benchmark, the $\sim 10\%$ uncertainty on the nucleon-level cross section, $\sigma(\nu_\mu n \to \mu^- p)|_{E_\nu = 1\,\mathrm{GeV}} = 10.1(0.9) \times 10^{-39}\,\mathrm{cm}^2$ due to axial form factor shape uncertainty already saturates the error budget of next generation experiments.[21] This situation motivates an improvement of elementary nucleon-level amplitudes from lattice QCD [112, 113, 119], from new precise neutrino data, and/or potential advances in other fields such as muon capture in muonic hydrogen [114]. More refined treatment of QED radiative corrections is also needed for neutrino experiments [41, 115].

5.2 Formal questions in effective field theory

Certain radiative corrections to nuclear structure effects contributing to muonic hydrogen demand consideration of the $1/M^4$ heavy particle lagrangian (NRQED) [116]. It is only at this order that an interplay of Lorentz and gauge symmetry causes a violation [117] of reparameterization invariance as implemented by a classic ansatz [118]. Muonic hydrogen helped uncover this interesting feature of effective field theory.

5.3 Nonperturbative methods

Lattice QCD offers a route to nucleon form factors that is independent of detector-dependent radiative corrections (although the impact of QED corrections to lattice predictions must be robustly estimated). In the context of the axial form factor, probed most directly in neutrino scattering, practical considerations (underground safety for hydrogen or deuterium targets) may also impede further experimental progress. Next generation lattice QCD is poised to contribute.[22] There are also novel methods under investigation to access the radii directly on the lattice, instead of using the form factor as intermediary [125].

The precision spectroscopy of muonic atoms heavier than hydrogen demands correspondingly precise nuclear structure calculations on light nuclei, and is a proving grounds for ab initio nuclear methods [126–129]. There is presently reasonable agreement between different methods for deuteron structure corrections, although (cf. Fig. 13) there remains an intriguing $\sim 2.5\sigma$ discrepancy between the deuteron radius measured in regular and muonic deuterium.

5.4 Fundamental constants

Taking the muonic hydrogen results at face value implies a shift in the Rydberg constant by $\sim 7\sigma$ [2, 4]. The proton charge radius is a well defined observable of Nature,[23] and again taking the muonic hydrogen result at face value, this observable will change by $\sim 7\sigma$ (correlated with the Rydberg).

5.5 Motivating searches for new phenomena

The proton radius puzzle has motivated a variety of investigations into possible phenomena beyond the Standard Model [130–136], part of the broader program of searching for violations of lepton universality and light, weakly-coupled new physics scenarios [137, 138]. The puzzle has also motivated

---

[21] Determination of the requisite nuclear corrections presently relies on data-driven modeling [97–101] employing experimental constraints [102–108]. Ab-initio nuclear computations are beginning to provide additional insight [109–111]. Regardless of whether nuclear corrections are constrained experimentally or derived from first principles, independent knowledge of the elementary nucleon-level amplitudes is essential.

[22] For recent work, see: [112, 113, 119–124].

[23] This observable is of course determined by the parameters appearing in the Standard Model lagrangian, by a relation that we cannot yet determine with the accuracy of the muonic hydrogen measurement.

novel perspectives on computations within the Standard Model; for a recent example see Refs. [139–141].

6 Outlook

Laser spectroscopy of light muonic atoms has acted as a disruptive technology, demanding and motivating the development of better theoretical tools, and instigating a range of new experimental measurements.

The extraction of the proton charge radius from electron scattering data remains a controversial topic. Within the quoted experimental uncertainties of the highest statistics dataset [40], and employing standard models for radiative corrections, the data prefer a value of r_E^p significantly higher than muonic hydrogen (cf. Fig. 4). It is straightforward to account for form factor nonlinearities (the proper treatment of these effects is essential, cf. the alarming discrepancy between the first two points in Fig. 4). At the same time it is critical to account for radiative corrections, both soft (model independent) and hard (model dependent). A complete calculation of the Sudakov-enhanced soft corrections (cf. Fig. 7) reveals deficiencies in previous treatments that are in tension with the assumed experimental error budget [40], but appear unlikely to solely account for the radius anomaly. The same calculation reveals an ambiguity in the treatment of hard TPE of similar magnitude. Of special interest are new measurements that can address remaining theoretical uncertainties, like hard two-photon exchange [142].

New electron scattering measurements focused on low Q^2 are anticipated to provide an alternative determination of r_E^p. While of fundamental importance, such measurements will not by themselves shed light on whether underestimated systematic effects are impacting the higher-Q^2 data (and whether such effects can be ignored in the low-Q^2 data). Similarly, several theoretical approaches employ a subset of the scattering data (typically at low-Q^2), and/or effectively overrule the scattering data with other constraints to find a charge radius consistent with muonic hydrogen. Irrespective of details, such approaches cannot by themselves explain the existing anomaly (which requires consideration of a broad Q^2 range, cf. Fig. 2), and cannot offer a satisfactory resolution to the proton radius puzzle.

This point becomes especially acute for the analog process of neutrino scattering, where both form factor shape and radiative corrections play an important role, and where quantitative control of cross sections over a broad range of Q^2 is critical for the global long baseline neutrino program. Here we do not have the luxury of restricting to small Q^2, or to enforcing constraints on spectral functions using the analog of precise e^+e^- hadron production data.

The structure-dependent TPE effect in muonic hydrogen has received significant attention from a variety of approaches (cf. Fig. 12). This contribution remains a dominant uncertainty in the determination of the r_E^p from muonic hydrogen, but new constraints on the subtraction function leave limited room for large effects (cf. Fig. 10, and Fig. 11 RHS).

The proton radius puzzle has motivated investigations leading to new formal results in effective field theory, surprises in seemingly well-established operator product expansions, and many new analyses of hadronic structure using a variety of effective field theories. New experimental efforts in the realm of lepton universality tests are coming online and promise yet further insights.

References

[1] P. J. Mohr, D. B. Newell and B. N. Taylor, Rev. Mod. Phys. **88**, no. 3, 035009 (2016). [arXiv:1507.07956 [physics.atom-ph]].

[2] A. Antognini *et al.*, Science **339**, 417 (2013).

[3] Pohl, R., Nez, F., Udem, T., et al. 2016, arXiv:1607.03165 (Metrologia, in press).

[4] P. J. Mohr, B. N. Taylor and D. B. Newell, Rev. Mod. Phys. **84**, 1527 (2012) [arXiv:1203.5425 [physics.atom-ph]].

[5] R. Pohl *et al.*, Nature **466**, 213 (2010).

[6] R. Pohl, R. Gilman, G. A. Miller and K. Pachucki, Ann. Rev. Nucl. Part. Sci. **63**, 175 (2013) [arXiv:1301.0905 [physics.atom-ph]].

[7] C. E. Carlson, Prog. Part. Nucl. Phys. **82**, 59 (2015) [arXiv:1502.05314 [hep-ph]].

[8] A. Beyer *et al.*, Annalen Phys. **525**, no. 8-9, 671 (2013).

[9] J. C. Bernauer *et al.* [A1 Collaboration], Phys. Rev. Lett. **105**, 242001 (2010) [arXiv:1007.5076 [nucl-ex]].

[10] X. Zhan *et al.*, Phys. Lett. B **705**, 59 (2011) [arXiv:1102.0318 [nucl-ex]].

[11] J. Arrington and I. Sick, J. Phys. Chem. Ref. Data **44**, 031204 (2015) [arXiv:1505.02680 [nucl-ex]].

[12] C. G. Parthey, A. Matveev, J. Alnis, R. Pohl, T. Udem, U. D. Jentschura, N. Kolachevsky and T. W. Hänsch, Phys. Rev. Lett. **104**, 233001 (2010).

[13] A. Matveev *et al.*, Phys. Rev. Lett. **110**, no. 23, 230801 (2013).

[14] C. G. Parthey *et al.*, Phys. Rev. Lett. **107**, 203001 (2011) [arXiv:1107.3101 [physics.atom-ph]].

[15] G. Lee, J. R. Arrington and R. J. Hill, Phys. Rev. D **92**, 013013 (2015) [arXiv:1505.01489 [hep-ph]].

[16] R. J. Hill and G. Paz, Phys. Rev. D **82**, 113005 (2010) [arXiv:1008.4619 [hep-ph]].

[17] B. Bhattacharya, R. J. Hill and G. Paz, Phys. Rev. D **84**, 073006 (2011) [arXiv:1108.0423 [hep-ph]].

[18] I. T. Lorenz and U. G. Meißner, Phys. Lett. B **737**, 57 (2014) [arXiv:1406.2962 [hep-ph]].

[19] Z. Epstein, G. Paz and J. Roy, Phys. Rev. D **90**, no. 7, 074027 (2014) [arXiv:1407.5683 [hep-ph]].

[20] B. Bhattacharya, G. Paz and A. J. Tropiano, Phys. Rev. D **92**, no. 11, 113011 (2015) [arXiv:1510.05652 [hep-ph]].

[21] For a review and further references see: R. J. Hill, *In the Proceedings of 4th Flavor Physics and CP Violation Conference (FPCP 2006), Vancouver, British Columbia, Canada, 9-12 Apr 2006, pp 027* [arXiv:hep-ph/0606023].

[22] C. Bourrely, B. Machet and E. de Rafael, Nucl. Phys. B **189**, 157 (1981).

[23] C. G. Boyd, B. Grinstein and R. F. Lebed, Phys. Rev. Lett. **74**, 4603 (1995) [arXiv:hep-ph/9412324].

[24] C. G. Boyd, B. Grinstein and R. F. Lebed, Nucl. Phys. B **461**, 493 (1996) [arXiv:hep-ph/9508211].

[25] L. Lellouch, Nucl. Phys. B **479**, 353 (1996) [arXiv:hep-ph/9509358].

[26] I. Caprini, L. Lellouch and M. Neubert, Nucl. Phys. B **530**, 153 (1998) [arXiv:hep-ph/9712417].

[27] C. M. Arnesen, B. Grinstein, I. Z. Rothstein and I. W. Stewart, Phys. Rev. Lett. **95**, 071802 (2005) [arXiv:hep-ph/0504209].

[28] T. Becher and R. J. Hill, Phys. Lett. B **633**, 61 (2006) [arXiv:hep-ph/0509090].

[29] R. J. Hill, Phys. Rev. D **74**, 096006 (2006) [arXiv:hep-ph/0607108].

[30] C. Bourrely, L. Lellouch and I. Caprini, Phys. Rev. D **79**, 013008 (2009) [arXiv:0807.2722 [hep-ph]].

[31] A. Bharucha, T. Feldmann and M. Wick, JHEP **1009**, 090 (2010) [arXiv:1004.3249 [hep-ph]].

[32] Y. Amhis *et al.* [Heavy Flavor Averaging Group (HFAG) Collaboration], arXiv:1412.7515 [hep-ex].

[33] C. Bouchard *et al.* [HPQCD Collaboration], Phys. Rev. D **88**, no. 5, 054509 (2013) [Phys. Rev. D **88**, no. 7, 079901 (2013)] [arXiv:1306.2384 [hep-lat]].

[34] J. A. Bailey *et al.*, Phys. Rev. D **93**, no. 2, 025026 (2016) [arXiv:1509.06235 [hep-lat]].

[35] R. R. Horgan, Z. Liu, S. Meinel and M. Wingate, Phys. Rev. D **89**, no. 9, 094501 (2014) [arXiv:1310.3722 [hep-lat]].

[36] J. A. Bailey *et al.* [Fermilab Lattice and MILC Collaborations], Phys. Rev. D **92**, no. 1, 014024 (2015) [arXiv:1503.07839 [hep-lat]].

[37] W. Detmold, C. Lehner and S. Meinel, Phys. Rev. D **92**, no. 3, 034503 (2015) [arXiv:1503.01421 [hep-lat]].

[38] B. Chakraborty *et al.* [HPQCD Collaboration], Phys. Rev. D **89**, no. 11, 114501 (2014) [arXiv:1403.1778 [hep-lat]].

[39] M. Distler, private communication.

[40] J. C. Bernauer *et al.* [A1 Collaboration], Phys. Rev. C **90**, no. 1, 015206 (2014) [arXiv:1307.6227 [nucl-ex]].

[41] R. J. Hill, Phys. Rev. D **95**, no. 1, 013001 (2017) [arXiv:1605.02613 [hep-ph]].

[42] R. J. Hill and G. Paz, Phys. Rev. Lett. **107**, 160402 (2011) [arXiv:1103.4617 [hep-ph]].

[43] M. Vanderhaeghen, J. M. Friedrich, D. Lhuillier, D. Marchand, L. Van Hoorebeke and J. Van de Wiele, Phys. Rev. C **62**, 025501 (2000) [hep-ph/0001100].

[44] W. A. McKinley and H. Feshbach, Phys. Rev. **74**, 1759 (1948).

[45] P. G. Blunden, W. Melnitchouk and J. A. Tjon, Phys. Rev. C **72**, 034612 (2005).

[46] P. G. Blunden, W. Melnitchouk and J. A. Tjon, Phys. Rev. Lett. **91**, 142304 (2003).

[47] C. E. Carlson and M. Vanderhaeghen, Ann. Rev. Nucl. Part. Sci. **57**, 171 (2007).

[48] J. Arrington, P. G. Blunden and W. Melnitchouk, Prog. Part. Nucl. Phys. **66**, 782 (2011).

[49] O. Tomalak, B. Pasquini and M. Vanderhaeghen, arXiv:1612.07726 [hep-ph].

[50] I. Sick, Prog. Part. Nucl. Phys. **67**, 473 (2012).

[51] I. Sick and D. Trautmann, Phys. Rev. C **89**, no. 1, 012201 (2014) [arXiv:1407.1676 [nucl-ex]].

[52] K. Griffioen, C. Carlson and S. Maddox, Phys. Rev. C **93**, no. 6, 065207 (2016) [arXiv:1509.06676 [nucl-ex]].

[53] M. Horbatsch and E. A. Hessels, Phys. Rev. C **93**, no. 1, 015204 (2016) [arXiv:1509.05644 [nucl-ex]].

[54] D. W. Higinbotham, A. A. Kabir, V. Lin, D. Meekins, B. Norum and B. Sawatzky, Phys. Rev. C **93**, no. 5, 055207 (2016) [arXiv:1510.01293 [nucl-ex]].

[55] E. Kraus, K. E. Mesick, A. White, R. Gilman and S. Strauch, Phys. Rev. C **90**, no. 4, 045206 (2014) [arXiv:1405.4735 [nucl-ex]].

[56] I. T. Lorenz, U. G. Meißner, H.-W. Hammer and Y.-B. Dong, Phys. Rev. D **91**, no. 1, 014023 (2015) [arXiv:1411.1704 [hep-ph]].

[57] M. Horbatsch, E. A. Hessels and A. Pineda, arXiv:1610.09760 [nucl-th].

[58] I. Sick and D. Trautmann, Phys. Rev. C **95**, no. 1, 012501 (2017) [arXiv:1701.01809 [nucl-ex]].

[59] M. A. Belushkin, H.-W. Hammer and U.-G. Meissner, Phys. Rev. C **75**, 035202 (2007) [hep-ph/0608337].

[60] M. Hoferichter, B. Kubis, J. Ruiz de Elvira, H.-W. Hammer and U.-G. Meißner, Eur. Phys. J. A **52**, no. 11, 331 (2016) [arXiv:1609.06722 [hep-ph]].

[61] R. J. Hill and G. Paz, arXiv:1611.09917 [hep-ph].

[62] M. C. Birse and J. A. McGovern, Eur. Phys. J. A **48**, 120 (2012) [arXiv:1206.3030 [hep-ph]].

[63] K. Pachucki, Phys. Rev. A **60**, 3593 (1999).

[64] G. A. Miller, Phys. Lett. B **718**, 1078 (2013) [arXiv:1209.4667 [nucl-th]].

[65] J. C. Collins, Nucl. Phys. B **149**, 90 (1979) Erratum: [Nucl. Phys. B **153**, 546 (1979)] Erratum: [Nucl. Phys. B **915**, 392 (2017)].

[66] A. P. Martynenko, Phys. Atom. Nucl. **69**, 1309 (2006). [hep-ph/0509236].

[67] D. Nevado and A. Pineda, Phys. Rev. C **77**, 035202 (2008). [arXiv:0712.1294 [hep-ph]].

[68] C. E. Carlson and M. Vanderhaeghen, Phys. Rev. A **84**, 020102 (2011). [arXiv:1101.5965 [hep-ph]].

[69] M. Gorchtein, F. J. Llanes-Estrada and A. P. Szczepaniak, Phys. Rev. A **87**, no. 5, 052501 (2013). [arXiv:1302.2807 [nucl-th]].

[70] J. M. Alarcon, V. Lensky and V. Pascalutsa, Eur. Phys. J. C **74**, no. 4, 2852 (2014). [arXiv:1312.1219 [hep-ph]].

[71] A. Antognini, F. Kottmann, F. Biraben, P. Indelicato, F. Nez and R. Pohl, Annals Phys. **331**, 127 (2013). [arXiv:1208.2637 [physics.atom-ph]].

[72] C. Peset and A. Pineda, Nucl. Phys. B **887**, 69 (2014). [arXiv:1406.4524 [hep-ph]].

[73] R. Pohl *et al.* [CREMA Collaboration], Science **353**, no. 6300, 669 (2016).

[74] A. Antognini *et al.*, Can. J. Phys. **89**, no. 1, 47 (2011).

[75] N. Nevo Dinur, C. Ji, S. Bacca and N. Barnea, Phys. Lett. B **755**, 380 (2016) [arXiv:1512.05773 [nucl-th]].

[76] O. J. Hernandez, N. Nevo Dinur, C. Ji, S. Bacca and N. Barnea, Hyperfine Interact. **237**, no. 1, 158 (2016) [arXiv:1604.06496 [nucl-th]].

[77] C. E. Carlson, M. Gorchtein and M. Vanderhaeghen, Phys. Rev. A **95**, no. 1, 012506 (2017) [arXiv:1611.06192 [nucl-th]].

[78] A. Beyer, L. Maisenbacher, K. Khabarova, C. G. Parthey, A. Matveev, J. Alnis, R. Pohl, N. Kolachevsky, Th. Udem and T. W. Hänsch, talk of R. Pohl at Hadronic Contributions to New Physics Searches, Tenerife, Spain, 25-30 September 2016.

[79] Antognini, A., Schuhmann, K., Amaro, F. D., et al., European Physical Journal Web of Conferences, **113**, 01006 (2016).

[80] Herrmann, M., Haas, M., Jentschura, U. D., et al., Phys. Rev. A **79**, 052505 (2009).

[81] Kandula, D. Z., Gohle, C., Pinkert, T. J., Ubachs, W., & Eikema, K. S. E., Phys. Rev. Lett. **105**, 063001.

[82] Morgenweg, J., Barmes, I., & Eikema, K. S. E., Nature Physics, **10**, 30 (2014).

[83] Liu, J., Salumbides, E. J., Hollenstein, U., et al., J. Chem. Phys. **130**, 174306 (2009).

[84] Schiller, S., Bakalov, D., & Korobov, V. I., Phys. Rev. Lett. **113**, 023004 (2014).

[85] Dickenson, G. D., Niu, M. L., Salumbides, E. J., et al., Phys. Rev. Lett. **110**, 193601 (2013).

[86] Biesheuvel, J., Karr, J.-P., Hilico, L., et al., Nature Communications, **7**, 10385 (2016).

[87] J.-P. Karr, L. Hilico, J. Koelemeij and V. Korobov, Phys. Rev. A **94**, no. 5, 050501 (2016) [arXiv:1605.05456 [physics.atom-ph]].

[88] U. D. Jentschura, P. J. Mohr, J. N. Tan and B. J. Wundt, Phys. Rev. Lett. **100**, 160404 (2008).

[89] Tan, J. N., Brewer, S. M., & Guise, N. D. 2011, Physica Scripta Volume T, **144**, 014009.

[90] A. Gasparian [PRad at JLab Collaboration], EPJ Web Conf. **73**, 07006 (2014).

[91] M. Mihovilovič *et al.*, arXiv:1612.06707 [nucl-ex].

[92] R. Gilman *et al.* [MUSE Collaboration], arXiv:1303.2160 [nucl-ex].

[93] A. Manohar, P. Nason, G. P. Salam and G. Zanderighi, Phys. Rev. Lett. **117**, no. 24, 242002 (2016) [arXiv:1607.04266 [hep-ph]].

[94] G. A. Fiorentini *et al.* [MINERvA Collaboration], Phys. Rev. Lett. **111**, 022502 (2013) [arXiv:1305.2243 [hep-ex]].

[95] A. S. Meyer, M. Betancourt, R. Gran and R. J. Hill, Phys. Rev. D **93**, no. 11, 113015 (2016) [arXiv:1603.03048 [hep-ph]].

[96] A. Bodek, S. Avvakumov, R. Bradford and H. S. Budd, Eur. Phys. J. C **53**, 349 (2008) [arXiv:0708.1946 [hep-ex]].

[97] C. Andreopoulos *et al.*, Nucl. Instrum. Meth. A **614**, 87 (2010) [arXiv:0905.2517 [hep-ph]].

[98] Y. Hayato, Acta Phys. Polon. B **40**, 2477 (2009).

[99] O. Buss *et al.*, Phys. Rept. **512**, 1 (2012) [arXiv:1106.1344 [hep-ph]].

[100] T. Golan, C. Juszczak and J. T. Sobczyk, Phys. Rev. C **86**, 015505 (2012) [arXiv:1202.4197 [nucl-th]].

[101] T. Katori and M. Martini, arXiv:1611.07770 [hep-ph].

[102] D. Drakoulakos *et al.* [MINERvA Collaboration], hep-ex/0405002.

[103] A. A. Aguilar-Arevalo *et al.* [MiniBooNE Collaboration], Phys. Rev. D **81**, 092005 (2010) [arXiv:1002.2680 [hep-ex]].

[104] A. A. Aguilar-Arevalo *et al.* [MiniBooNE Collaboration], Phys. Rev. D **83**, 052007 (2011) [arXiv:1011.3572 [hep-ex]].

[105] A. A. Aguilar-Arevalo *et al.* [MiniBooNE Collaboration], Phys. Rev. D **82**, 092005 (2010) [arXiv:1007.4730 [hep-ex]].

[106] K. Abe *et al.* [T2K Collaboration], Phys. Rev. D **91**, no. 7, 072010 (2015) [arXiv:1502.01550 [hep-ex]].

[107] C. Anderson *et al.* [ArgoNeuT Collaboration], Phys. Rev. Lett. **108**, 161802 (2012) [arXiv:1111.0103 [hep-ex]].

[108] P. A. Rodrigues *et al.* [MINERvA Collaboration], [arXiv:1511.05944 [hep-ex]].

[109] A. Lovato, S. Gandolfi, R. Butler, J. Carlson, E. Lusk, S. C. Pieper and R. Schiavilla, Phys. Rev. Lett. **111**, no. 9, 092501 (2013) [arXiv:1305.6959 [nucl-th]].

[110] S. Bacca and S. Pastore, J. Phys. G **41**, no. 12, 123002 (2014) [arXiv:1407.3490 [nucl-th]].

[111] J. Carlson, S. Gandolfi, F. Pederiva, S. C. Pieper, R. Schiavilla, K. E. Schmidt and R. B. Wiringa, arXiv:1412.3081 [nucl-th].

[112] A. S. Meyer, R. J. Hill, A. S. Kronfeld, R. Li and J. N. Simone, arXiv:1610.04593 [hep-lat].

[113] B. Yoon *et al.*, arXiv:1611.07452 [hep-lat].

[114] V. A. Andreev *et al.* [MuCap Collaboration], Phys. Rev. Lett. **110**, no. 1, 012504 (2013) [arXiv:1210.6545 [nucl-ex]].

[115] M. Day and K. S. McFarland, Phys. Rev. D **86**, 053003 (2012) [arXiv:1206.6745 [hep-ph]].

[116] R. J. Hill, G. Lee, G. Paz and M. P. Solon, Phys. Rev. D **87**, 053017 (2013) [arXiv:1212.4508 [hep-ph]].

[117] J. Heinonen, R. J. Hill and M. P. Solon, Phys. Rev. D **86**, 094020 (2012) [arXiv:1208.0601 [hep-ph]].

[118] M. E. Luke and A. V. Manohar, Phys. Lett. B **286**, 348 (1992) [hep-ph/9205228].

[119] T. Bhattacharya, V. Cirigliano, S. Cohen, R. Gupta, H. W. Lin and B. Yoon, Phys. Rev. D **94**, no. 5, 054508 (2016) [arXiv:1606.07049 [hep-lat]].

[120] M. Abramczyk *et al.* [RBC and UKQCD Collaborations], arXiv:1610.09773 [hep-lat].

[121] T. Yamazaki [PACS Collaboration], PoS LATTICE **2015**, 081 (2016) [arXiv:1511.09179 [hep-lat]].

[122] J. Liang, Y. B. Yang, K. F. Liu, A. Alexandru, T. Draper and R. S. Sufian, arXiv:1612.04388 [hep-lat].

[123] A. Abdel-Rehim *et al.*, Phys. Rev. D **92**, no. 11, 114513 (2015) Erratum: [Phys. Rev. D **93**, no. 3, 039904 (2016)] [arXiv:1507.04936 [hep-lat]].

[124] D. Djukanovic, T. Harris, G. von Hippel, P. Junnarkar, H. B. Meyer and H. Wittig, arXiv:1611.07918 [hep-lat].

[125] C. Alexandrou, arXiv:1612.04644 [hep-lat].

[126] R. Machleidt, Phys. Rev. C **63**, 024001 (2001) [nucl-th/0006014].

[127] J. L. Friar, Phys. Rev. C **88**, no. 3, 034003 (2013) [arXiv:1306.3269 [nucl-th]].

[128] O. J. Hernandez, C. Ji, S. Bacca, N. Nevo Dinur and N. Barnea, Phys. Lett. B **736**, 344 (2014) [arXiv:1406.5230 [nucl-th]].

[129] K. Pachucki and A. Wienczek, Phys. Rev. A **91**, no. 4, 040503 (2015) [arXiv:1501.07451 [physics.atom-ph]].

[130] V. Barger, C. W. Chiang, W. Y. Keung and D. Marfatia, Phys. Rev. Lett. **106**, 153001 (2011) [arXiv:1011.3519 [hep-ph]].

[131] D. Tucker-Smith and I. Yavin, Phys. Rev. D **83**, 101702 (2011) [arXiv:1011.4922 [hep-ph]].

[132] B. Batell, D. McKeen and M. Pospelov, Phys. Rev. Lett. **107**, 011803 (2011) [arXiv:1103.0721 [hep-ph]].

[133] C. E. Carlson and B. C. Rislow, Phys. Rev. D **86**, 035013 (2012) [arXiv:1206.3587 [hep-ph]].

[134] C. E. Carlson and B. C. Rislow, Phys. Rev. D **89**, no. 3, 035003 (2014) [arXiv:1310.2786 [hep-ph]].

[135] V. Pauk and M. Vanderhaeghen, Phys. Rev. Lett. **115**, no. 22, 221804 (2015) [arXiv:1503.01362 [hep-ph]].

[136] Y. S. Liu, D. McKeen and G. A. Miller, Phys. Rev. Lett. **117**, no. 10, 101801 (2016) [arXiv:1605.04612 [hep-ph]].

[137] D. Bryman, W. J. Marciano, R. Tschirhart and T. Yamanaka, Ann. Rev. Nucl. Part. Sci. **61**, 331 (2011).

[138] See: http://redtop.fnal.gov.

[139] C. P. Burgess, P. Hayman, M. Rummel and L. Zalavari, arXiv:1612.07337 [hep-ph].

[140] C. P. Burgess, P. Hayman, M. Williams and L. Zalavari, arXiv:1612.07313 [hep-ph].

[141] C. P. Burgess, P. Hayman, M. Rummel, M. Williams and L. Zalavari, arXiv:1612.07334 [hep-ph].

[142] B. Henderson *et al.* [OLYMPUS Collaboration], arXiv:1611.04685 [nucl-ex].